Cylindrical versus Spherical Micelle Formation in Block Copolymer/Homopolymer Blends

Anne M. Mayes* and Monica Olvera de la Cruz

Department of Materials Science and Engineering, Northwestern University, 2145 Sheridan Road, Evanston, Illinois 60208. *Received September 3, 1987; Revised Manuscript Received November 23, 1987*

ABSTRACT: Micelle formation in dilute solutions of A–B diblock copolymer in homopolymer A is studied. The effects of varying copolymer block lengths and homopolymer molecular weight on micelle morphology are analyzed. The minimum concentration required for the formation of micelles is determined for cylindrical and spherical micelles. A trend toward cylinder formation is observed with increasing B block fraction and increasing homopolymer molecular weight.

Introduction

Blends of a block copolymer with a homopolymer possess unique mechanical and rheological properties.[1–6] As a consequence of a net repulsive interaction between components in the system, these mixtures form a rich variety of morphologies.[1–6] Even in the simplest example of a dilute solution of A–B diblock copolymer in homopolymer A, incompatibility between A and B can give rise to the formation of copolymer aggregates within a homopolymer-rich matrix.[4–6] These aggregates, or micelles, are characterized by a core that is rich in component B and an outer shell composed of homopolymer chains mixed with the A block of the copolymer.

A number of experimental[4–6] and theoretical[7–10] studies have been made on micelle formation in diblock copolymer/homopolymer systems. Rigby and Roe[5] used small-angle X-ray scattering (SAXS) to study micelle formation in mixtures of styrene–butadiene diblock copolymer with butadiene homopolymer by varying temperature, copolymer concentration, and relative block lengths. Kinning and Thomas[6] studied dilute poly(styrene–butadiene)/polystyrene systems via SAXS and transmission electron microscopy. They observed changes in micelle morphology from spherical to nonspherical micelle geometries by changing the butadiene block fraction or homopolymer molecular weight.

Several authors have developed models for micelle formation by minimizing the free energy of the system.[7,9,10] All assume a spherical micelle geometry, neglecting the possibility of more favored morphologies. In particular, changes from spherical to cylindrical micelles are observed even in dilute solutions.[6] The potential to create in situ fiber composites by using only dilute concentrations of copolymer makes cylindrical micelle formation an attractive technological pursuit.

Here we propose a model for cylindrical micelle formation in dilute A–B diblock copolymer/A homopolymer solutions to determine what conditions favor cylindrical micelle geometry over spheres. Free energy expressions for spherical and cylindrical micelles are minimized. We analyze changes in shape and size of the micelles as a function of concentration and molecular weight. We compare the minimum copolymer concentration required for micelle formation for the two geometries under identical conditions. We hereafter refer to the minimum copolymer concentration as the critical micelle concentration, although we do not imply that sharp transitions are exhibited in micelle formation.

Description of the Model

Let N and N_h be the number of statistical segments in the A–B diblock copolymer and A homopolymer, respectively. (For simplicity we assume the symmetric case, where A and B segments have equal persistence length, a.) Let f be the A-block fraction of the copolymer, and $\alpha = N/N_h$. Consider a dilute concentration φ of copolymer in the homopolymer. We assume that a net repulsive interaction between A and B monomers will give rise to the formation of copolymer aggregates. Two morphologies of the aggregates will be considered: spherical and cylindrical micelles. We construct the free energy of the system of micelles for each morphology with respect to the state where homopolymers and block copolymers are not mixed. To ensure that the copolymer chains in the blend obey Gaussian statistics, we restrict α to values less than $N^{1/2}$.[11] In addition, to assure thermodynamic equilibrium, the A block must be larger than N_h, therefore $\alpha > 1/f$.[7,10,12]

Geometries for the spherical and cylindrical micelles are shown in Figure 1. To maintain simplicity, the ends of the cylinders are taken to be flat. We assume a sharp interface exists between the core, which contains the B monomers, and the outer shell. The quantity η is the fraction of monomers in the outer shell contributed by the A block of the copolymer. The remainder of the shell ($1 - \eta$) is composed of interpenetrating homopolymer chains. For both geometries the total radius $R = R_B + R_A$, where R_B is the radius of the core and R_A is the outer shell radius. L is the length of the cylinder. The system is considered to be monodisperse, each micelle containing p copolymer chains.

Assuming that for a dilute concentration of copolymer the interactions between the micelles can be neglected,[12] the total free energy of a system of micelles is described in analogy to the model proposed by Leibler, Orland, and Wheeler[10] (LOW) as

$$F_{tot} = nF + F_{mix} - TS_m \quad (1)$$

where F is the free energy of a single micelle, n is the number of micelles in the system, and F_{mix} is the Flory–Huggins free energy of mixing for the homopolymer and block copolymer chains which remain outside the micelles. S_m is the translational entropy of the micelles in the system. S_m will be lower for cylindrical micelles, which contain many more chains per micelle than the spheres.

The micelle free energy F is comprised of four contributions. Let us first consider how these contributions affect the geometry of the micelles. The first contribution is the interfacial tension present at the A–B interface, σ. The interfacial area per copolymer chain is reduced by forming large aggregations of copolymer chains and therefore tends to favor the formation of long cylinders over spheres. In the spheres, large aggregations are limited by the deformation energy, F_d. Deformation energy results from contracting or elongating the copolymer chains from their unperturbed dimensions by confining them to a characteristic micelle geometry. For example, if copolymer

0024-9297/88/2221-2543$01.50/0

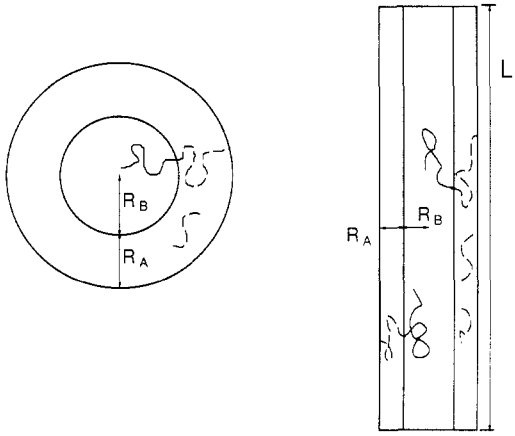

Figure 1. Schematic cross-sections for spherical and cylindrical micelles. Inner core of radius R_B contains only B monomers. Outer shell of radius R_A contains A monomers from homopolymer and A blocks of copolymer. L is length of cylinder.

chains are added to the micelle, as a result of incompressibility the B blocks in the core of the sphere must stretch to accommodate the new chains. In the cylindrical geometry, however, the additional degree of freedom along the axis allows many chains to be incorporated into the structure without significant changes in chain configuration. Thus the chains in the core of the cylinder are expected to remain relaxed, while those in the sphere are stretched unfavorably. The deformational contribution to the free energy is largely responsible for the transition from spherical to cylindrical micelles.

A third contribution to the micelle free energy is the joint localization energy, F_j. This term arises from the decrease in entropy associated with fixing the A–B joint of the block copolymer at the interface. Localization energy favors fewer chains per micelle and therefore discourages cylinder formation.

The final contribution to the micelle free energy is the mixing entropy of the homopolymer and A blocks of the copolymer in the outer shell of the micelle, F_m. The mixing entropy is increased by increasing the amount of homopolymer in the shell. If the concentration of homopolymer becomes too large, however, the A blocks will be elongated, which is energetically unfavorable. It is primarily the balance of these two effects which determines the morphology of the outer shell.

Considering the above contributions to the free energy, the general equation for the free energy of a single micelle is

$$F = A_i\sigma + F_d + F_m + F_j \qquad (2)$$

where A_i is the interfacial area. The interfacial tension is approximated as

$$\sigma = (kT/a^2)(\chi/6)^{1/2} \qquad (3)$$

where χ is the Flory interaction parameter.[13] This expression holds for a narrow, planar, A–B interface. Curvature effects are expected to be negligibly small, of the order a/R_B.[14]

Table I lists explicit expressions for the four terms which compose F. The localization energy, F_j, is obtained by first imagining that the A blocks of copolymer are ideally mixed with the homopolymer chains in the outer shell volume, V_s. (F_m consequently includes both terms in the Flory–Huggins free energy expression.) One end segment of each A block chain (the A–B joint) is then confined to a site on the interface, increasing the free energy by $kTp \ln (V_s/A_i a)$, the joint localization energy. (An equivalent expression for $F_j + F_m$ may be obtained by first localizing the A–B joint with respect to the volume of the A blocks only, ηV_s. The free energy of mixing, F_m, will then contain only the contribution of the homopolymer chains.)

Table I
Contributions to Micelle Free Energy

	Sphere
$A_i\sigma$	$4\pi R_B^2 \frac{kT}{a^2}\left(\frac{\chi}{6}\right)^{1/2}$
F_j	$kTp \ln\left(\frac{R^3 - R_B^3}{3R_B^2 a}\right)$
F_m	$\frac{4\pi}{3a^3}(R^3 - R_B^3)\, kT\left\{\frac{\eta}{N_A}\ln\eta + \frac{(1-\eta)}{N_h}\ln(1-\eta)\right\}$
F_d	$kTp\left\{\frac{3}{2}\frac{R_A^2}{Nfa^2} + \frac{3}{2}\frac{R_B^2}{N(1-f)a^2} + \frac{\pi^2 Nfa^2}{6R_A^2} + \frac{\pi^2 N(1-f)a^2}{6R_B^2} - 6.29\right\}$
	Cylinder
$A_i\sigma$	$2\pi R_B L \frac{kT}{a^2}\left(\frac{\chi}{6}\right)^{1/2}$
F_j	$kTp \ln\left(\frac{R^2 - R_B^2}{2R_B a}\right)$
F_m	$\frac{\pi}{a^3}(R^2 - R_B^2)LkT\left\{\frac{\eta}{N_A}\ln\eta + \frac{(1-\eta)}{N_h}\ln(1-\eta)\right\}$
F_d	$kTp\left\{\frac{3}{2}\frac{R_A^2}{Nfa^2} + \frac{3}{2}\frac{R_B^2}{N(1-f)a^2} + \frac{(2.40)^2}{6}\frac{N(1-f)a^2}{R_B^2} + \frac{\pi^2 Na^2}{6L^2} - 4.92\right\}$

In Table I we have listed approximate expressions for the deformation energy F_d of both systems. For the chains in the core, we have calculated the probability that a B chain which begins with one end fixed at the interface, and is constrained to remain in the volume of the core, will end at a point r after $(1-f)N$ steps.[7,15,16] In order to find the most probable value of r, we maximize the probability. We then calculate the decrease in entropy with respect to the ideal configuration in the unmixed state. We have considered the limiting cases, $R_B^2/(1-f)Na^2 > 1$ and $R_B^2/(1-f)Na^2 < 1$, of the expressions obtained; that is, we have ignored the logarithmic terms in the deformation energy.[8-10]

Analogous calculations were carried out for deformation energy of the A block chains. In the cylindrical case, there are no linear contributions to the decrease in entropy of the form fNa^2/R_A^2.[15] Instead the decrease in entropy in the limit $R_A^2/fNa^2 < 1$ is linear in fNa^2/R_B^2,[16] which is absorbed in the term Na^2/L^2.

Having arrived at an expression for the free energy of a single micelle, we have left only to consider the remaining two terms in the total free energy expression (1):

$$F_{mix} = kT(1 - \varphi\gamma\Lambda)\left\{\frac{\varphi_1}{N}\ln\varphi_1 + \frac{(1-\varphi_1)}{N_h}\ln(1-\varphi_1) + (1-f)\chi\varphi_1[1-(1-f)\varphi_1]\right\} \qquad (4)$$

$$S_m = -k\Omega\left\{\frac{\varphi\gamma}{pN}\ln(\varphi\gamma\Lambda) + \frac{1-\varphi\gamma\Lambda}{pN}\ln(1-\varphi\gamma\Lambda)\right\} \quad (5)$$

where φ is the concentration of copolymers in the solution, γ is the fraction of copolymer monomers which aggregate to form micelles, and φ_1 is the concentration of copolymer monomers in the volume outside the micelles, given by

$$\varphi_1 = \frac{\varphi(1-\gamma)}{1-\varphi\gamma\Lambda} \quad (6)$$

with

$$\Lambda = \frac{f}{\eta} + 1 - f \quad (7)$$

The total number of monomers in the system is given by Ω, so that the number of micelles, n, can be written as $\Omega\varphi\gamma/pN$. The translational entropy of the micelles given by (5) is obtained from a lattice of cells, each with the volume of a single micelle. Within this approximation eq 4 and 5 are independent of the geometry of the micelles.

To characterize the system of micelles, we solve for the equilibrium values of the chosen parameters by minimizing the free energy with respect to each parameter.[10] In the system of spheres, we minimize F as a function of p, η, and γ by relating the micelle geometry to p and η through incompressibility conditions

$$pfNa^3 = \frac{4}{3}\pi R_B^3 \quad (8)$$

$$pN\Lambda a^3 = \frac{4}{3}\pi R^3 \quad (9)$$

For the case of the cylinders, the equilibrium length of the micelle creates an additional unknown. We must, therefore, minimize the total free energy of the system with respect to four parameters in order to completely characterize the system. We use the parameters p, η, γ, and R_B and apply the incompressibility conditions

$$pfNa^3 = \pi R_B^2 L \quad (10)$$

$$pN\Lambda a^3 = \pi R^2 L \quad (11)$$

The two systems of M equation/M unknown nonlinear equations obtained through the minimization procedure were solved numerically through an iterative procedure to five significant figures.

Results and Discussion

We studied the effects of homopolymer molecular weight on micelle morphology by varying the ratio $\alpha = N/N_h$ while keeping the number of block copolymer segments N fixed. As α increases, the homopolymer chains become shorter, increasing the entropy of mixing outside the micelles,[10] so that less copolymer chains aggregate into micelles. Also, shorter homopolymer chains cause a gain in mixing entropy of the A blocks with the homopolymer in the outer shell so that it becomes increasingly swollen with homopolymer.

Behavior analogous to increasing α is observed when the interaction χN is decreased. As χN decreases, keeping α and f constant, the concentration of homopolymer in the outer shell $(1-\eta)$ increases and fewer chains aggregate into micelles. Decreasing χN even further, the reverse effect is observed for $(1-\eta)$; i.e., in the low segregation limit, as χN decreases $(1-\eta)$ starts decreasing. A maximum in $(1-\eta)$ as a function of α also occurs when α is sufficiently large. The effects on $(1-\eta)$ when α increases (or χN decreases) are reflected in the outer shell radius.

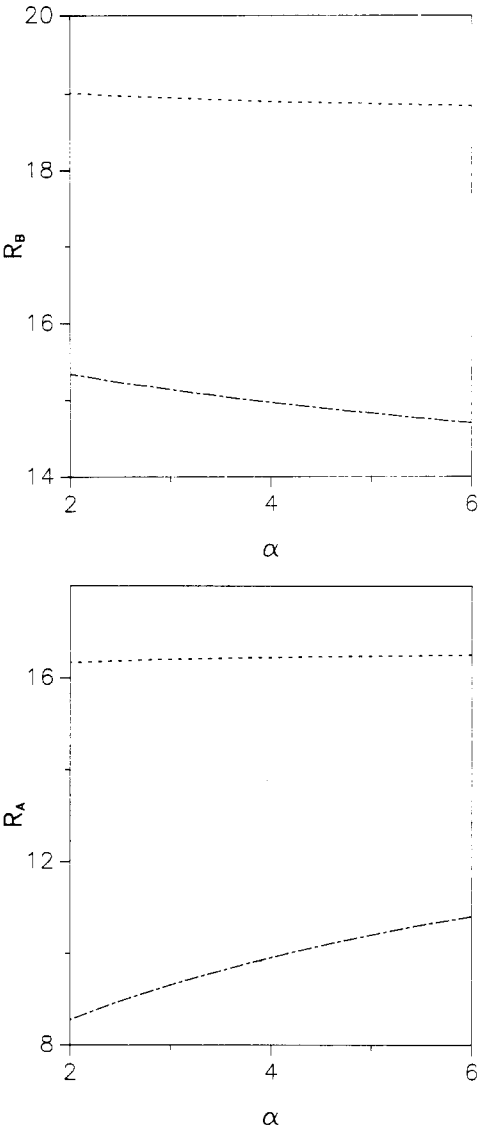

Figure 2. (a, top) Sphere (---) and cylinder (– -) core radius R_B versus α for $f = 0.5$, $\varphi = 0.1$, $N = 500$, and $\chi = 0.04$. The unperturbed rms end-to-end distance is 15.81, in units of the monomer persistence length a. (b, bottom) Sphere (---) and cylinder (– -) outer shell radius R_A.

In Figure 2, the A and B components of the micelle radius are shown as a function of α for both geometries, with $f = 0.5$ and χN and φ constant. The copolymer chain configurations in both the core and the shell are remarkably different for the two geometries. In the core of the sphere, the B chains are notably elongated from their Gaussian configuration. (For $fN = 250$, the unperturbed root mean squared (rms) end-to-end distance is $15.81a$). Increasing the homopolymer molecular weight (decreasing α) causes the B chains to stretch further as more chains are collected into the structure. In contrast, B blocks in the cylinder are slightly contracted from their unperturbed dimensions. When α decreases, more chains add to the cylinder, decreasing the interfacial area per copolymer chain and relaxing the chains in the core. This large contrast in chain deformation between the sphere and the cylinder can induce a change in morphology from spheres to cylinders by increasing homopolymer molecular weight.

The A blocks in the cylinder and the sphere also show distinctly different behavior (Figure 2b). In the sphere, A blocks stretch slightly to accommodate large concentrations of homopolymer in the shell ($\eta < 0.2$). The cylinder contains a much smaller homopolymer fraction (η

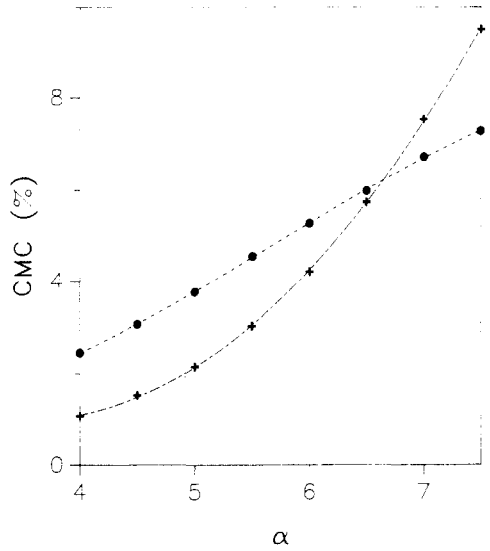

Figure 3. Cmc as a function of α for $\chi = 0.05$, $N = 400$, and $f = 0.5$. A trend toward cylinder formation with decreasing α is observed. Sphere (●); cylinder (+).

> 0.4). Instead the chains tend to collapse along the length of the cylinder in order to minimize the deformation energy (Table I).

Since we have neglected the free energy contribution from the ends of the cylinder, the model cannot describe the actual transition from spherical to cylindrical micelles. Nevertheless, by comparing the minimum concentration of copolymer required for micelle formation in the two geometries under identical conditions, we obtain the trends we expect to observe in dilute systems of block copolymer with homopolymer.

Figure 3 shows critical micelle concentration (cmc) as a function of α for $f = 0.5$ and $\chi N = 20$. For low homopolymer molecular weights, or large α, the critical micelle concentration is much higher for the cylinders than for the spheres, indicating that formation of the spheres is favored. As the homopolymer chains become longer, the cmc decreases due to an increase in the entropy of mixing in the system. For the cylindrical geometry, the cmc drops off sharply. At low values of α, the cylinders reveal lower cmc values than the spheres. Thus comparison of the cmc values indicates a trend toward cylindrical micelle formation when the molecular weight of the homopolymer solvent is increased. For lower values of χN, both geometries display an expected decrease in cmc. LOW discussed this matter in some detail for the case of spheres, and we find similar results for the cylinder morphology.

Changes in micelle morphology can additionally take place in dilute solutions by varying the block lengths of the copolymer. We examined the effects of varying the B block length while the number of segments in the A block and the homopolymer were kept constant. Figure 4 gives the cmc results for $N_A = 200$ and $N_h = 50$. As the size of the B block is increased, or $f = N_A/N$ is decreased, the cmc is lowered, while the number of chains per micelle increases. Again, we observe stretching of the B chains in the sphere, while those in the core of the cylinder are relaxed. At low values of f, the cmc values are lower in the cylinders than in the spheres, and we expect the cylinders to be favored.

The same trend is exhibited when the length of the B block and the homopolymer are fixed, while the number of segments in the A block is varied (Figure 5). As the length of the A block increases, the solubility of the block copolymer in the homopolymer improves. Thus a larger concentration of copolymer is required to form micelles,

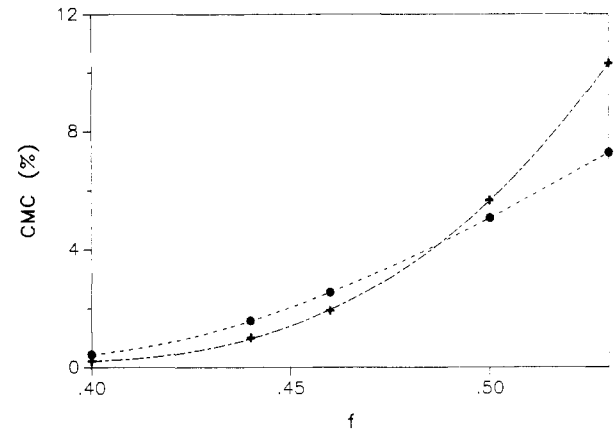

Figure 4. Cmc as a function of f for $N_A = 200$, $N_h = 50$, and $\chi = 0.055$. A trend toward cylinder formation with decreasing f is observed. Sphere (●); cylinder (+).

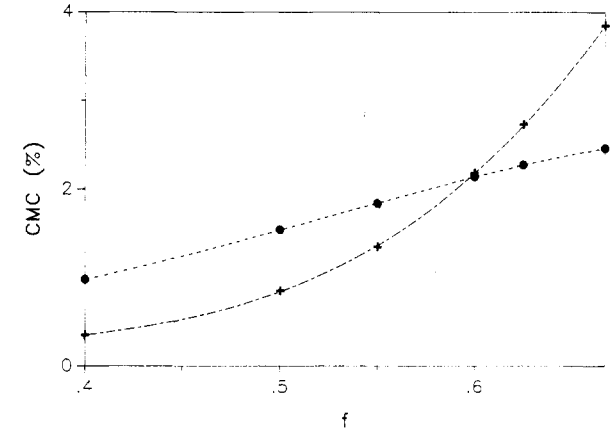

Figure 5. Cmc as a function of f for $N_B = 300$, $N_h = 100$, and $\chi = 0.04$. A trend toward cylinder formation with decreasing f is observed. Sphere (●); cylinder (+).

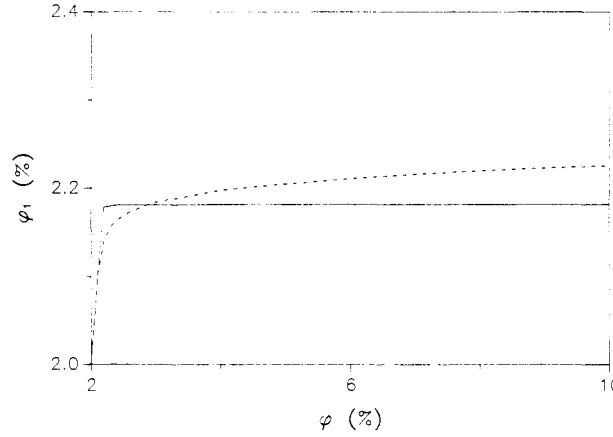

Figure 6. Copolymer concentration in the volume outside the micelles φ_1, as a function of φ for $\chi N = 30$, $f = 0.6$, and $\alpha = 7.5$. Sphere (- - -); cylinder (—).

and the number of copolymer chains per micelle decreases. As the A block length is reduced, a change in morphology to cylindrical micelles takes place.

More insight into the nature of micelle formations can be gained by examining the effects of copolymer concentration on morphology. Figure 6 depicts the copolymer concentration in the volume outside the micelles, φ_1, as a function of the total copolymer concentration in the system. As φ is increased beyond the critical micelle concentration, the spheres show a gradual increase in φ_1; that is, some of the chains which are added to the system do not aggregate. This behavior indicates that micelle for-

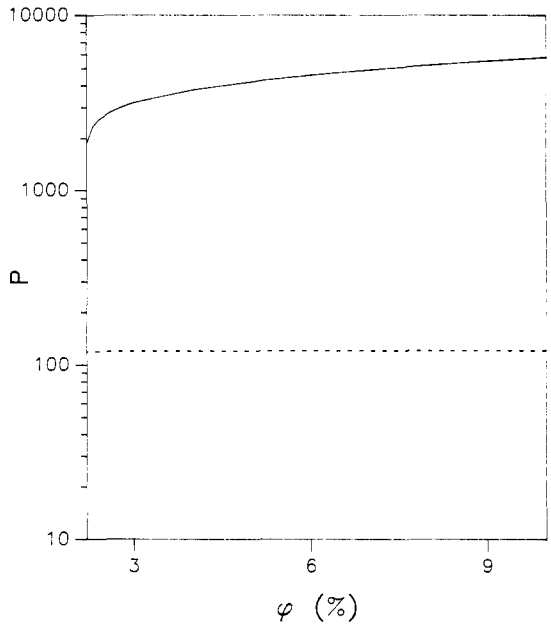

Figure 7. Chains per micelle (p) as a function of φ for $\chi N = 30$, $f = 0.6$, and $\alpha = 7.5$. Dramatic increase in p is found for cylinders as φ increases. Sphere (---); cylinder (—).

mation is not a sharp transition, as previously discussed by LOW. Those chains which do aggregate tend to form new micelles rather than add to existing ones. Thus, only a slight increase is seen in the number of chains per micelle as the concentration increases (Figure 7).

In the cylinders, an increase in φ_1 can barely be detected as φ increases beyond the cmc. Figure 7 shows that increasing the concentration results in a large increase in the number of chains per micelle. The additional degree of freedom in the cylinders allows chains to be added to the existing micelles without the configurational energy penalties imposed on the spheres. It suggests that sphere to cylinder transitions may also take place by increasing the concentration of copolymer in the system. As previously stated, this model does not apply for larger concentrations of block copolymer. When the concentration of block copolymer increases, the distance between micelles decreases. The interaction between micelles might give rise to micellular ordered structures.[4-7,12,17]

Changes from spherical to cylindrical micelle formations in dilute poly(styrene–butadiene)/polystyrene solutions were observed experimentally by Kinning and Thomas.[6] Using transmission electron microscopy, they found wormlike micelle structures were formed by increasing the molecular weight of the butadiene block or the homopolystyrene. These results are in agreement with the trends shown in Figures 3 and 4. For reasons previously discussed, we do not expect the cmc crossovers to represent true transition points. In particular, we have neglected the ends of the cylinder so that cylinder formation will be prematurely favored by the model. In addition, we have assumed that a uniform number of chains per micelle minimizes the free energy in monodisperse polymer samples.[18] Also, it should be kept in mind that other nonspherical morphologies could be favored over cylinders as the molecular weight of the B block or the homopolymer is increased further.

Acknowledgment. We are grateful to David J. Kinning for helpful discussions and for sending us his Ph.D. thesis. This work has been supported by the National Science Foundation through the Northwestern University Materials Research Center Grant DMR 8520280.

References and Notes

(1) Reiss, G.; Kohler, J.; Tournut, C.; Banderet, A. *Makromol. Chem.* **1967**, *101*, 58.
(2) Inoue, T.; Soen, T.; Hashimoto, T.; Kawai, H., *J. Polym. Sci., Polym. Chem. Ed.* **1969**, *7*, 1283. Inoue, T.; Soen, T.; Hashimoto, T.; Kawai, H. *Macromolecules* **1970**, *3*, 87. Hashimoto, T.; Shibayama, M.; Kawai, H. *Macromolecules* **1980**, *13*, 1237.
(3) Skoulios, A.; Helffer, P.; Gallot, Y.; Selb, J. *Makromol. Chem.* **1971**, *148*, 305.
(4) Ramon, A. R.; Cohen, R. E. *Polym. Eng. Sci.* **1977**, *17*, 639. Cohen, R. E.; Ramon, A. R. *Macromolecules* **1979**, *12*, 313. Cohen, R. E.; Wilfond, D. E. *Macromolecules* **1982**, *15*, 370. Bates, F. S.; Bernoy, C. V.; Cohen, R. E. *Macromolecules* **1983**, *16*, 1101.
(5) Roe, R. J.; Zin, W. C. *Macromolecules* **1980**, *13*, 1221. Rigby, O.; Roe, R. J. *Macromolecules* **1984**, *17*, 1778; *Macromolecules* **1986**, *19*, 721.
(6) (a) Kinning, D. J. Ph.D. Thesis, University of Massachusetts, Amherst, 1986. (b) Kinning, D. J.; Thomas, E. L. *Structural Studies of Micelles in Block Copolymer/Homopolymer Blends*; preprint; Parts I and II.
(7) Meier, D. J. *J. Polym. Sci., Part C* **1969** 26, 81; *Polym. Prepr. (Am. Chem. Soc., Div. Polym. Chem.)* **1970**, *11*, 400; **1977**, *18*, 340, 837.
(8) de Gennes, P.-G. In *Solid State Physics*; Liebert, L., Ed.; Academic: New York, 1978; Suppl. 14.
(9) Noolandi, J.; Hong, M. K. *Macromolecules* **1982**, *15*, 482. Whitmore, M. D.; Noolandi, J. *Macromolecules* **1985**, *18*, 657.
(10) Leibler, L.; Orland, H.; Wheeler, J. C. *J. Chem. Phys.* **1983**, *79*, 3550.
(11) de Gennes, P.-G. *Scaling Concepts in Polymer Physics*; Cornell University Press: Ithaca, NY, 1979.
(12) Leibler, L.; Pincus, P. A. *Macromolecules* **1984**, *17*, 2922.
(13) Helfand, E.; Tagami, Y. *J. Polym. Sci., Part B* **1971**, *9*, 741. Helfand, E.; Sapse, A. M. *J. Chem. Phys.* **1975**, *62*, 1327. Helfand, E.; Wasserman, Z. R. *Macromolecules* **1976**, *9*, 879.
(14) Rowlinson, J. S.; Widom, B. *Molecular Theory of Capillarity*; Clarendon: Oxford, 1982.
(15) Semenov, A. N. *Sov. Phy. JETP* **1985**, *61* (4), 733.
(16) Carslaw, H. S.; Jaeger, J. C. *Conduction of Heat in Solids*, 2nd ed.; Oxford University Press: London, 1959; pp 198–199, 233, 331, 335–336, 366–370.
(17) Olvera de la Cruz, M.; Sanchez, I. *Macromolecules* **1987**, *20*, 440.
(18) Goldstein, R. E. *J. Chem. Phys.* **1986**, *84*, 3367.